Templated Synthesis of Amphiphilic Nanoparticles at the Liquid–Liquid Interface

Dickson M. Andala, Sun Hae Ra Shin, Hee-Young Lee, and Kyle J. M. Bishop*

Department of Chemical Engineering, The Pennsylvania State University, University Park, Pennsylvania 16802, United States

ABSTRACT

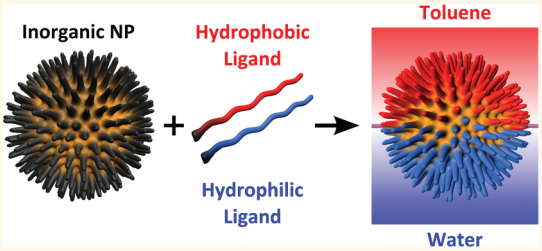

A simple and reliable method is described to produce inorganic nanoparticles functionalized asymmetrically with domains of hydrophobic and hydrophilic ligands on their respective hemispheres. These amphiphilic, Janus-type particles form spontaneously by a thermodynamically controlled process, in which the particle cores and two competing ligands assemble at the interface between two immiscible liquids to reduce the interfacial energy. The asymmetric surface chemistry resulting from this process was confirmed using contact angle measurements of water droplets on nanoparticle monolayers deposited onto hydrophobic and hydrophilic substrates—particles presenting their hydrophobic face give contact angles of ~96°, those presenting their hydrophilic face ~19°. The spontaneous assembly process is rationalized by a thermodynamic model, which accounts both for the energetic contributions driving the assembly and for the entropic penalties that must be overcome. Consistent with the model, amphiphilic NPs form only when there is sufficient interfacial area to accommodate them; however, this potential limitation is easily overcome by mechanical agitation of the two-phase mixture. While it is straightforward to vary the ratio of hydrophobic and hydrophilic ligands, the accumulation of amphiphilic particles at the interface is maximal for ligand ratios near 1:1. In addition to gold nanoparticles and thiolate ligands, we demonstrate the generality of this approach by extending it to the preparation of amphiphilic iron oxide nanoparticles using two types of diol-terminated ligands. Depending on the material properties of the inorganic cores, the resulting amphiphilic particles should find applications as responsive particle surfactants that respond dynamically to optical (plasmonic particles) and/or magnetic (magnetic particles) fields.

KEYWORDS: self-assembly · Janus particle · mixed monolayer · surfactants · responsive · spontaneous

The ability to functionalize nanoscale colloids with a desired distribution of hydrophobic and hydrophilic surface regions remains an outstanding challenge in materials chemistry. Like molecular amphiphiles (*e.g.*, surfactants and peptides[1]), amphiphilic particles are desirable both as surface-active agents[2] and for their propensity to self-assemble[3] into higher order aggregates, including well-defined clusters,[4,5] disk-shaped[6,7] and cylindrical[8,9] micelles, colloidosomes,[10] and lattices,[11] through the use of directional interactions.[12,13] Unlike their molecular analogues, however, amphiphiles incorporating nanoscopic, inorganic cores allow for additional functionalities such as superparamagnetism,[14] plasmonic excitation,[15] and enhanced fluorescence[16] among others. Unfortunately, there exists no general synthetic strategy by which to prepare such "responsive" nanoparticles possessing amphiphilic surfaces. By contrast, the preparation of micrometer-scale Janus particles[17] is readily achieved by immobilizing particles at an interface (solid–air,[4,11,18–20] solid–liquid,[22,23] liquid–liquid[10]) and chemically modifying their exposed surface, for example, by metal vapor deposition,[4,11,18–20] electroless plating,[22] microcontact printing,[21] or particle lithography.[23] For smaller nanoscale particles, such methods are generally less effective owing to the rotational diffusion of the particles (the rate of which scales as $\sim d^{-3}$ where d is the particle diameter); therefore, alternative strategies based on spontaneous self-organization are preferred. For example, nanoparticle alloys[24] and core–shell[25] particles can phase separate to form dumbbell-shaped heterodimers composed of two different materials fused together;[13,17,25,26] similar behaviors have been demonstrated using block copolymer micelles.[27] Alternatively, nanoparticles with "patchy" surfaces but homogeneous cores can be prepared through the phase separation of immiscible ligands bound to the particles' surface.[5–7,28,29] Importantly, the geometry of the phase-separated domains can, in principle, be controlled by templating monolayer segregation at a fluid interface.[30]

Building on this concept, we describe a general strategy for the amphiphilic functionalization of gold nanoparticles

* Address correspondence to kjmbishop@engr.psu.edu.

Received for review July 8, 2011 and accepted January 3, 2012.

Published online January 03, 2012
10.1021/nn202556b

based on their *spontaneous* organization at a liquid–liquid interface through the segregation of hydrophobic and hydrophilic ligands bound to the particles' surface. Unlike previous strategies that rely on mixed monolayers[31,32] to produce Pickering-type surfactants[2,33] with homogeneous surface chemistries, our approach yields Janus-type particles with amphiphilic surfaces. Furthermore, asymmetric surface functionalization does not rely on particle immobilization.[34] Instead, we demonstrate that the desired amphiphilic particles correspond to the thermodynamically favored arrangement of the system's components. As described by a simple thermodynamic model, the assembly process is driven by the reduction in interfacial energy and depends on both the concentration of NPs in the mixture and on the ratio of the competing ligands. Finally, we demonstrate how this approach can be extended to other nanoparticle–ligand chemistries by preparing amphiphilic nanoparticles with iron oxide cores.

RESULTS AND DISCUSSION

Gold nanoparticles (NPs) 9.2 ± 1.2 nm in diameter were synthesized according to a modified literature procedure.[35,36] Initially, the particles were stabilized by weakly bound dodecylamine (DDA) ligands and dispersed in the toluene phase of a toluene–water mixture (cf. Figure 1a). Simultaneous addition of an equal number of two competing ligands—one hydrophobic (dodecanethiol, DDT), the other hydrophilic (mercaptoundecanoic acid, MUA; fully deprotonated at pH = 11)—followed by vigorous agitation resulted in the accumulation of the newly functionalized particles at the water–toluene interface as verified by UV–vis measurements on the respective bulk phases (Figure 1b). At the interface, the color of NPs changed noticeably from red to purple due to surface plasmon coupling between proximal particles; specifically, the absorbance maximum, λ_{max}, increased from 523 nm in solution to ~540 nm at the interface (cf. Supporting Information, section 2 for details). Once formed, these surface-active NPs remained stable for months without particle merging as verified by TEM. Additionally, the resulting NP surfactants could be dried and redispersed without compromising their surface activity (cf. Supporting Information, section 3).

Importantly, the propensity of the particles to accumulate at the interface relies on the presence of *both* DDT and MUA ligands. Addition of DDT ligands alone produced NPs that were fully soluble in toluene and completely insoluble in water; conversely, the addition of MUA ligands alone produced water-soluble NPs that were completely insoluble in toluene. Owing to the large differences in solubility between the two ligands in the respective phases, we hypothesized that the surface-active NPs were not covered uniformly by a mixed monolayer of DDT and MUA ligands but rather

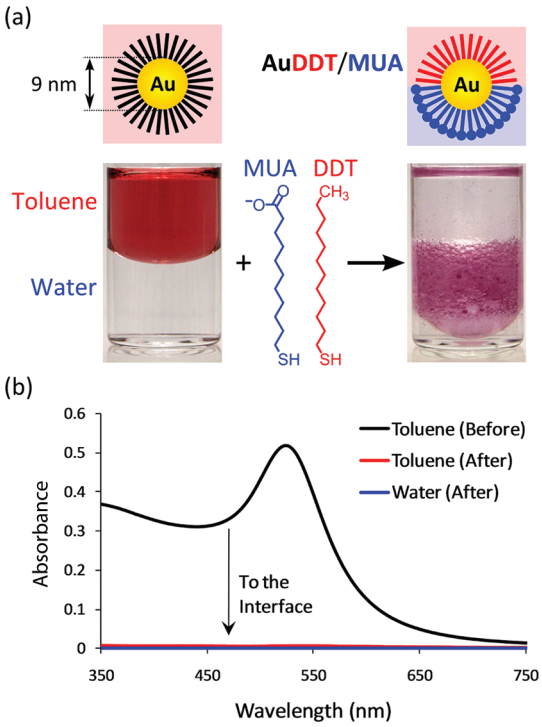

Figure 1. (a) Schematic illustration of the surface functionalization procedure. The combination of AuNPs with hydrophobic (DDT) and hydrophilic (MUA) ligands in a toluene–water mixture yields amphiphilic nanoparticles at the liquid–liquid interface. The rightmost image shows water droplets covered with NPs. For clarity, the schematic illustration of AuDDT/MUA shows complete segregation between the respective ligands. While some degree of asymmetric functionalization is certain (cf. Figure 2), the precise extent of phase separation between DDT and MUA ligands is unknown. (b) UV–vis spectra of the NP solutions before and after functionalization show that nanoparticles, initially present in the toluene phase, assemble at the interface with no particles remaining in either bulk phase.

asymmetrically, with the water side enriched in negatively charged MUA ligands and the toluene side enriched in hydrophobic DDT ligands.

To test this hypothesis, we performed contact angle measurements of water droplets on different surfaces coated with the functionalized NPs (Figure 2). Specifically, we prepared silicon substrates functionalized with self-assembled monolayers (SAMs) of (*i*) 3-(trihydroxysilyl)-1-propanesulfonic acid (hydrophilic substrate; Figure 2a) and (*ii*) trimethoxy(octyl)silane (hydrophobic substrate; Figure 2d). To facilitate the interaction between the negatively charged carboxylate groups on the NPs with those on hydrophilic substrates, the latter were coordinated with Zn^{2+} ions by immersion in an aqueous solution of zinc chloride ($[ZnCl_2]$ = 0.01 M). Amphiphilic, surface-active NPs were then deposited onto both hydrophobic and hydrophilic substrates by dip coating to yield high density NP monolayers as verified by SEM (Figure 2c,f).

Prior to the deposition of the NPs, the contact angles of water droplets deposited onto the hydrophilic and hydrophobic substrates were 15 and 95°, respectively

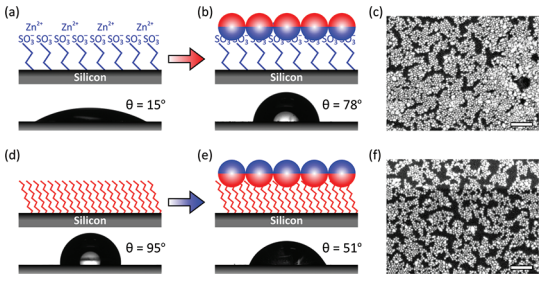

Figure 2. Contact angle measurements. (a) Hydrophilic substrate created by the silanization of an oxidized silicon surface with 3-(trihydroxysilyl)-1-propane sulfonic acid followed by immersion in an aqueous solution of zinc chloride 0.01 M. The measured contact angle of water in air is 15 ± 2.3° as illustrated in the photo. (b) Amphiphilic NP monolayers deposited onto the hydrophilic substrate in (a). The measure contact angle is 78 ± 2.2°. (c) SEM image of an NP monolayer deposited onto the hydrophilic substrate *via* dip coating. Scale bar is 100 nm. (d) Hydrophobic substrate created by the silanization of an oxidized silicon surface with trimethoxy(octyl)silane. The measured contact angle is 95 ± 2.3°. (e) Amphiphilic NP monolayers deposited onto the hydrophobic substrate in (d). The measure contact angle is 51 ± 1.5°. (f) SEM image of an NP monolayer deposited onto the hydrophobic substrate. Scale bar is 100 nm.

(Figure 2a,d). Deposition of amphiphilic NPs onto hydrophilic substrates increased the apparent contact angle of the surface to 78° (Figure 2b); deposition of identical NPs onto hydrophobic substrates decreased the contact angle to 51° (Figure 2e). Importantly, the measured contact angles for the NP monolayers were dependent on the chemical functionality of the underlying substrate, suggesting that NPs were asymmetrically functionalized with MUA and DDT ligands. Specifically, NPs deposited onto hydrophobic substrates present hydrophilic MUA ligands and yield smaller contact angles than identical NPs deposited onto hydrophilic substrates, which present hydrophobic DDT ligands.

While some degree of asymmetric functionalization is certain, the precise extent to which DDT and MUA ligands segregate between the two hemispheres of the NPs' surface is less clear. SEM images of the NP-coated substrates reveal a chemically heterogeneous surface (Figure 2c,f) of which ~70% is covered by bifunctional NPs and the remaining ~30% by the underlying SAM. The measured contact angles thus reflect contributions from *both* of these regions as approximated by Cassie's law:[37] $\cos\theta = f_{NP}\cos\theta_{NP} + (1 - f_{Np})\cos\theta_0$, where θ is the measured contact angle, f_{NP} is the fractional coverage of NPs (here, $f_{NP} \sim 0.70$), θ_{NP} is the contact angle of a close-packed NP monolayer, and θ_0 is the original contact angle prior to the deposition of the particles. Using this relation, we estimate the "true" contact angle for NPs presenting DDT ligands (Figure 2b) to be $\theta_{NP} \approx 96°$; similarly, for NPs presenting MUA ligands (Figure 2e), $\theta_{NP} \approx 19°$. These values are similar to those of AuDDT nanoparticle monolayers ($\theta_{NP} \approx 110°$; cf. Supporting Information, section 4) and AuMUA nanoparticle monolayers ($\theta_{NP} \approx 23°$; cf. Supporting Information, section 4), respectively.

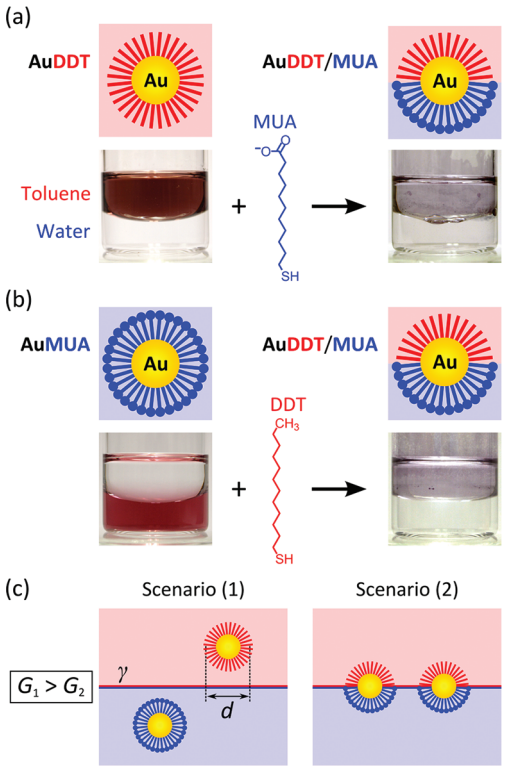

Figure 3. Thermodynamic considerations. (a) Formation of amphiphilic NPs is independent of the manner in which they are prepared. In one preparation, DDT ligands are added first, followed by MUA ligands. (b) In another, MUA ligands are added first, followed by DDT ligands. Both preparations yield the same amphiphilic NPs. In both (a) and (b), the initial NP concentration is 0.2 mM in 4 mL of toluene or 4 mL of water, respectively. (c) Formation of amphiphilic NPs at the liquid−liquid interface is a spontaneous process. In other words, the free energy *G* of scenario 2 is less than that of the alternative scenario 1.

Therefore, when the chemical heterogeneity of the surfaces is taken into account, contact angle measurements suggest that hydrophobic and hydrophilic ligands are highly segregated on the NPs' surface.

Regardless of the precise degree of ligand segregation, the assembly of particle cores and competing ligands at the toluene−water interface occurs spontaneously through a thermodynamically controlled process. To demonstrate this, we varied the order in which the MUA and DDT ligands were added and compared the resulting amphiphilic particles (Figure 3). In one case, DDT ligands were added first to create toluene soluble particles (Figure 3a); in another, MUA ligands were added first to create water-soluble particles (Figure 3b). Addition of the remaining ligand followed by vigorous shaking for 30 min gave amphiphilic particles that were indistinguishable from one another provided the final amounts of each ligand added were the same. To demonstrate this, we prepared monolayers of NPs functionalized through different preparations on both hydrophilic and hydrophobic substrates. The contact angles of water droplets on the resulting NP monolayers were identical to those presented in

Figure 2 to within experimental error (cf. Supporting Information, section 5 for details). Consequently, the propensity for NPs to assemble at the interface can be rationalized through thermodynamic arguments.

To show this, we approximate and compare the relative free energies of the following scenarios (Figure 3c): (1) in which NPs are partitioned equally between the bulk phases and covered uniformly with a single type of ligand (either AuMUA or AuDDT particles), and (2) in which all NPs are located at the interface and covered asymmetrically with MUA and DDT ligands (AuMUA-DDT particles). To simplify our estimate, we assume that MUA and DDT ligands are soluble only in the water and toluene phases, respectively. Furthermore, we limit our analysis to the symmetric case, in which the number of hydrophobic and hydrophilic ligands, their respective binding energies, and the volumes of the two phases are equal. With these assumptions, the difference between the chemical potentials of NPs in scenarios 1 and 2 can be approximated as follows (cf. Supporting Information, section 6 for a detailed derivation).

$$\mu_2 - \mu_1 \approx -\frac{1}{4}\pi d^2\gamma + k_B T \ln\left(\frac{2V}{Ad - Nd^3}\right) \quad (1)$$

Here, d is the particle diameter, γ is a characteristic surface energy of the toluene–water interface[38] ($\gamma \sim 40$ mJ/m^2), k_BT is the thermal energy, V is the volume of each bulk phase, A is the interfacial area between them, and N is the total number of NPs in the system. The first term describes the decrease in energy accompanying the formation of amphiphilic NPs, which effectively reduces the area of the toluene–water interface. The second describes the decrease in entropy associated with the NPs' loss of translational freedom upon transferring to the interface from the respective bulk phases (additional entropic contributions are discussed in the Supporting Information).

Importantly, the spontaneous formation of amphiphilic NPs can be favorable ($\mu_2 - \mu_1 < 0$) or unfavorable ($\mu_2 - \mu_1 > 0$) depending on the parameters of the system. For example, typical experimental parameters ($d = 9.2$ nm, $V = 4$ mL, $A = 6$ cm^2, $\gamma = 40$ mJ/m^2, and $N_o = 4 \times 10^{12}$ assuming a gold concentration of 0.04 mM) result in free energy differences of $\Delta\mu \approx -650 k_BT$ per NP, that is, negative in sign and large in magnitude. Consequently, the formation of amphiphilic particles localized at the toluene–water interface is thermodynamically favorable in qualitative agreement with the experimental observations.

Equation 1 also predicts that the formation of amphiphilic particles should depend on the area of toluene–water interface. At some point as the number of particles is increased, the interfacial area can no longer accommodate all of the particles, namely, when $Nd^2/A > 1$. Experimentally, this is illustrated in Figure 4a, which shows the results of experiments using different NP concentrations. In the first ($V = 3$ mL, $A = 6$ cm^2, and [AuNP] = 0.04 mM, corresponding to $Nd^2/A \sim 0.4$), the number of NPs is low, and they all organize at the interface to form amphiphilic particles. As the concentration is increased ($Nd^2/A > 1$), the toluene–water interface can no longer accommodate all of the particles, which then spread onto the glass–toluene interface to form dense coatings (presumably of similar amphiphilic NPs).

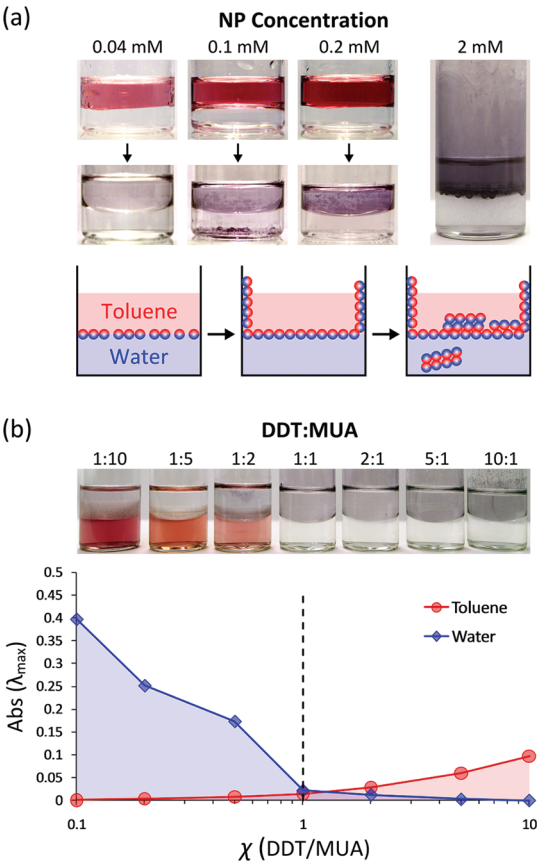

Figure 4. Effect of varying the NP concentration and ligand ratio. (a) At low concentrations (here, [AuNP] = 0.04 mM on a gold basis), NPs organize exclusively at the toluene–water interface. As the concentration is increased ([AuNP] = 0.1 and 0.2 mM), amphiphilic NPs coat the walls of the glass vials within the toluene phase. At high concentrations ([AuNP] = 2 mM), amphiphilic NPs, formed under vigorous agitation, aggregate at the interface and on the surface of the glass but remain largely insoluble in either bulk phase. The relevant experimental parameters are $V = 3$ mL and $A = 6$ cm^2. (b) UV–vis absorbance of the surface plasmon resonance (SPR) band at $\lambda_{max} = 525$ nm for NPs in water and $\lambda_{max} = 600$ nm for aggregated NPs in toluene as a function of the ligand ratio, χ. The concentration of NPs remaining in both bulk phase is minimal for $\chi = 1$.

When the NP concentration is very high (relative to the available interfacial area, *e.g.*, $Nd^2/A \sim 20$ in the rightmost image of Figure 4a), most of the NPs remain dissolved in the respective bulk phases, that is, AuMUA NPs in water and AuDDT NPs in toluene. Following the formation of a single monolayer of NPs at the interface, the creation of additional amphiphilic NPs is not thermodynamically favorable, requiring a spontaneous increase in the interfacial area. Nevertheless, it is still possible to

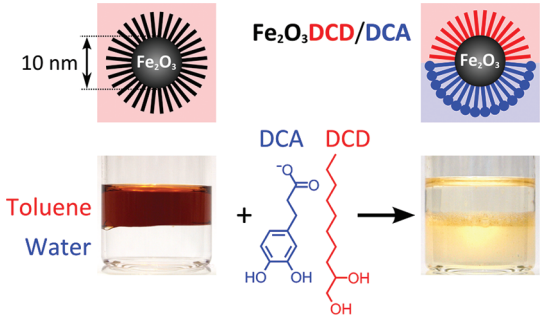

Figure 5. Extension to iron oxide NPs. The same methodology can also be applied to iron oxide NPs using hydrophobic (DCD) and hydrophilic (DCA) diol ligands. The turbidity of the aqueous phases after functionalization derives from small toluene droplets remaining therein (even after several hours of centrifugation); unlike analogous AuNPs, the amphiphilic iron oxide particles form highly stable emulsions.

drive *all* particles to accumulate at the interface by vigorously agitating the two-phase mixture to increase the interfacial area (Figure 4a). In the absence of continued agitation, however, the resulting emulsion gradually breaks (over the course of ~1 h), and the NPs aggregate onto the interface. Interestingly, the particles resulting from this "kinetic" preparation remain largely insoluble in either bulk phase for long periods (up to weeks) before gradually redispersing. Thus, while the mixed SAMs of hydrophobic and hydrophilic ligands do indeed redistribute themselves in time, the rate of this process is highly variable and depends on the local environment surrounding each particle (*e.g.*, formation of amphiphilic particles occurs in minutes; their disassembly within NP aggregates can take weeks).

In addition to the NP concentration, the spontaneous assembly of amphiphilic NPs at the toluene–water interface also depends on the ratio, χ, between the number of hydrophobic DDT ligands and hydrophilic MUA ligands in solution. As shown in Figure 4b, NPs accumulated at the interface for all values of χ investigated (0.1 to 10); however, the amount of NPs remaining in either bulk phase varied as the ligand ratio deviated from 1:1. Specifically, when MUA ligands were added in excess, some NPs remained dispersed in the aqueous phase; similarly, some NPs remained in the toluene phase in the presence of excess DDT ligands. The total amount of NPs remaining in both phases combined was minimal for ligand ratios of *ca.* 1:1. Furthermore, while NPs remaining in the aqueous phase for $\chi < 1$ were well-dispersed (due to stabilizing electrostatic forces), those found in the tolune phase for $\chi > 1$ showed signs of aggregation (namely, a red shift in the UV–vis absorption peak from 525 to 600 nm).

Finally, we note that this general functionalization strategy is not limited to AuNPs and thiolate ligands but should instead be applicable to any nanoparticle systems for which chemical ligation methods are well developed. To demonstrate this generality, we extended the present approach to synthesize amphiphilic iron oxide nanoparticles (7.5 ± 0.9 nm in diameter) using a similar combination of hydrophobic (1,2-decanediol, DCD) and hydrophilic (dihydrocinnamic acid, DCA; fully deprotonated at pH = 11) ligands (Figure 5). Interestingly, the emulsions formed during the synthesis of amphiphilic iron oxide particles (*i.e.*, following the agitation of the two phase NP/ligand mixtures) were highly stable and did not break within a month's time without prolonged centrifugation or addition of acid to protonate the DCA ligands. While the origins of this behavior remain uncertain, it may originate from (*i*) the use of short, divalent ligands, which allow the NPs to pack closer together within interfacial monolayers, and/or (*ii*) additional magnetic interactions between the NPs, which should further stabilize the NP monolayers separating the two phases.

CONCLUSIONS

In sum, we have developed a simple and reliable method for the synthesis of amphiphilic, inorganic NPs based on the spontaneous organization of particle cores and competing ligands to reduce the interfacial free energy between two immiscible liquids. We are currently applying this method to prepare particle surfactants, whose surface activity can be modulated by external fields, for example, plasmonic particles by optical illumination and ferrite particles by external magnetic fields. Of particular interest is the preparation of magnetic amphiphiles, for which the orientation of the particles' asymmetric surface functionality can be modulated dynamically through the rotation of its magnetic moment. Such responsive amphiphiles could find applications as mediators of temporary emulsions[39] and as "breathable" membranes[40] with dynamically tunable porosity. Additionally, by varying the relative amounts of particles and ligands, it should also be possible to control the hydrophilic–lipophilic balance of the particles and thereby their propensity to organize into various micellar assemblies. One challenge, or potential opportunity, remains: to understand, control, and apply the dynamic nature of the mixed SAMs decorating the functionalized NPs, which can reconfigure themselves in response to changes in the particles environment.

EXPERIMENTAL SECTION

Materials. Ultrapure grade tetra-*n*-butylammonium borohydride (TBAB), 1-dodecanethiol (DDT, 98%), tetramethylammonium hydroxide ($N(CH_3)_4OH$, 25% solution in methanol), trimethylamine *n*-oxide dihydrate, 3-(3,4-dihydroxyphenyl)propionic acid (dihydrocinnamic acid, DCA), and zinc chloride were obtained from

Alfa Aesar. 11-Mercaptoundecanoic acid (MUA, 99%) was obtained from Asemblon; dodecylamine (DDA) from Across; didodecyldimethylammonium bromide (DDAB) from Sigma Aldrich; gold chloride trihydrate crystal ($HAuCl_4 \cdot 3H_2O$) from J.T. Baker; iron pentacarbonyl from Strem Chemicals; 1,2-dodecanediol (DCD) from 3B Scientific; silicon wafers from Silicon Inc.; dioctyl ether from Spectrum Chemicals; trimethoxy(octyl)silane from Sigma Aldrich; 3-trihydroxysilylpropane sulfonic acid from Gelest Inc.; acetone, methanol, dichloromethane (CH_2Cl_2), oleic acid, and toluene from EMD Chemicals. All reagents were all used without further purification.

Nanoparticle Synthesis and Functionalization. Precursor solutions of AuNPs covered with dodecylamine (AuDDA) were prepared according to a slightly modified literature procedure,[31,35] in which $HAuCl_4 \cdot 3H_2O$ was used instead of $AuCl_3$ to obtain AuDDA particles dispersed in toluene with average diameters of 9.2 ± 1.2 nm (see Figure S1 of the Supporting Information). In a typical preparation of amphiphilic AuMUA-DDT NPs, 2 mL of toluene containing 0.4 μmol AuDDA (on a metal atom basis) was added to 2 mL of deionized water. To this mixture were injected simultaneously 0.02 μmol of MUA (dissolved in 0.1 mL of toluene) and 0.02 μmol of DDT (dissolved in 0.1 mL of toluene) to obtain a molar ratio of 20:1:1 for Au/MUA/DDT. After vigorous shaking and/or sonication for 30 min, the pH was adjusted to 11 by dropwise addition of an aqueous solution of tetramethyl ammonium hydroxide. After further shaking, the emulsified mixture was allowed to break, leaving amphiphilic NPs organized at the interface.

Similarly, γ-Fe_2O_3 nanoparticles were prepared using a literature procedure[41] to give 7.5 ± 0.9 nm particles dispersed in toluene and stabilized by oleic acid (see Figure S2 of the Supporting Information). As with the AuNPs, the as-prepared iron oxide particles were dispersed in the toluene phase of a toluene–water mixture, to which equal amounts of 1,2-decanediol (DCD) and dihydrocinnamic acid (DCA) were injected simultaneously to give a diol/Fe_2O_3 ratio of 1:10. The mixture was agitated vigorously for 30 min to drive the formation of amphiphilic NPs at the interface.

Characterization. UV–visible spectra were recorded on a Perkin-Elmer Lambda 35 UV–vis spectrometer over the range of 300–800 nm using a quartz cuvette (1 cm path length) and interfaced with UV WinLab software for data analysis. Scanning electron microscopy (SEM) was done on a JEOL 6700F FESEM at 3.0 kV on samples supported on Si wafer. Transmission electron microscopy (TEM) measurements were taken on JEOL JEM 1200 EXII operating at 80 kV accelerating voltage and attached to high-resolution Tietz F224 camera for image collection. TEM samples were drop cast onto a carbon-coated copper grid and allowed to dry at ambient conditions. Measurements of advancing contact angles were performed using a Ramé-Hart model 250 standard goniometer interfaced with DROPimage advanced software version 2.5.

Acknowledgment. K.J.M.B. gratefully acknowledges financial support from the Penn State Center for Nanoscale Science (NSF-MRSEC).

Supporting Information Available: TEM characterization of the gold and iron oxide nanoparticles; UV–vis characterization of NP monolayers; drying and redispersal of NP surfactants; additional contact angle measurements; detailed derivation and discussion of the thermodynamic model. This material is available free of charge *via* the Internet at http://pubs.acs.org.

REFERENCES AND NOTES

1. Cui, H. G.; Webber, M. J.; Stupp, S. I. Self-Assembly of Peptide Amphiphiles: From Molecules to Nanostructures to Biomaterials. *Biopolymers* **2010**, *94*, 1–18.
2. Binks, B. P. Particles as Surfactants—Similarities and Differences. *Curr. Opin. Colloid Interface Sci.* **2002**, *7*, 21–41.
3. Bishop, K. J. M.; Wilmer, C. E.; Soh, S.; Grzybowski, B. A. Nanoscale Forces and Their Uses in Self-Assembly. *Small* **2009**, *5*, 1600–1630.
4. Hong, L.; Cacciuto, A.; Luijten, E.; Granick, S. Clusters of Amphiphilic Colloidal Spheres. *Langmuir* **2008**, *24*, 621–625.
5. Wang, B. B.; Li, B.; Dong, B.; Zhao, B.; Li, C. Y. Homo- and Hetero-Particle Clusters Formed by Janus Nanoparticles with Bicompartment Polymer Brushes. *Macromolecules* **2010**, *43*, 9234–9238.
6. Jakobs, R. T. M.; van Herrikhuyzen, J.; Gielen, J. C.; Christianen, P. C. M.; Meskers, S. C. J.; Schenning, A. Self-Assembly of Amphiphilic Gold Nanoparticles Decorated with a Mixed Shell of Oligo(*p*-phenylene vinylene)s and Ethyleneoxide Ligands. *J. Mater. Chem.* **2008**, *18*, 3438–3441.
7. van Herrikhuyzen, J.; Portale, G.; Gielen, J. C.; Christianen, P. C. M.; Sommerdijk, N.; Meskers, S. C. J.; Schenning, A. Disk Micelles from Amphiphilic Janus Gold Nanoparticles. *Chem. Commun.* **2008**, 697–699.
8. Hartgerink, J. D.; Beniash, E.; Stupp, S. I. Self-Assembly and Mineralization of Peptide-Amphiphile Nanofibers. *Science* **2001**, *294*, 1684–1688.
9. Zubarev, E. R.; Xu, J.; Sayyad, A.; Gibson, J. D. Amphiphilicity-Driven Organization of Nanoparticles into Discrete Assemblies. *J. Am. Chem. Soc.* **2006**, *128*, 15098–15099.
10. Jiang, S.; Granick, S. Controlling the Geometry (Janus Balance) of Amphiphilic Colloidal Particles. *Langmuir* **2008**, *24*, 2438–2445.
11. Chen, Q. A.; Bae, S. C.; Granick, S. Directed Self-Assembly of a Colloidal Kagome Lattice. *Nature* **2011**, *469*, 381–384.
12. Zhang, Z. L.; Glotzer, S. C. Self-Assembly of Patchy Particles. *Nano Lett.* **2004**, *4*, 1407–1413.
13. Wei, Y. H.; Bishop, K. J. M.; Kim, J.; Soh, S.; Grzybowski, B. A. Making Use of Bond Strength and Steric Hindrance in Nanoscale "Synthesis". *Angew. Chem., Int. Ed.* **2009**, *48*, 9477–9480.
14. Batlle, X.; Labarta, A. Finite-Size Effects in Fine Particles: Magnetic and Transport Properties. *J. Phys. D: Appl. Phys.* **2002**, *35*, R15–R42.
15. Eustis, S.; El-Sayed, M. A. Why Gold Nanoparticles Are More Precious Than Pretty Gold: Noble Metal Surface Plasmon Resonance and Its Enhancement of the Radiative and Nonradiative Properties of Nanocrystals of Different Shapes. *Chem. Soc. Rev.* **2006**, *35*, 209–217.
16. Resch-Genger, U.; Grabolle, M.; Cavaliere-Jaricot, S.; Nitschke, R.; Nann, T. Quantum Dots *versus* Organic Dyes as Fluorescent Labels. *Nat. Methods* **2008**, *5*, 763–775.
17. Perro, A.; Reculusa, S.; Ravaine, S.; Bourgeat-Lami, E. B.; Duguet, E. Design and Synthesis of Janus Micro- and Nanoparticles. *J. Mater. Chem.* **2005**, *15*, 3745–3760.
18. Takei, H.; Shimizu, N. Gradient Sensitive Microscopic Probes Prepared by Gold Evaporation and Chemisorption on Latex Spheres. *Langmuir* **1997**, *13*, 1865–1868.
19. Paunov, V. N.; Cayre, O. J. Supraparticles and "Janus" Particles Fabricated by Replication of Particle Monolayers at Liquid Surfaces Using a Gel Trapping Technique. *Adv. Mater.* **2004**, *16*, 788–791.
20. Pawar, A. B.; Kretzschmar, I. Patchy Particles by Glancing Angle Deposition. *Langmuir* **2008**, *24*, 355–358.
21. Cayre, O.; Paunov, V. N.; Velev, O. D. Fabrication of Asymmetrically Coated Colloid Particles by Microcontact Printing Techniques. *J. Mater. Chem.* **2003**, *13*, 2445–2450.
22. Cui, J. Q.; Kretzschmar, I. Surface-Anisotropic Polystyrene Spheres by Electroless Deposition. *Langmuir* **2006**, *22*, 8281–8284.
23. Snyder, C. E.; Yake, A. M.; Feick, J. D.; Velegol, D. Nanoscale Functionalization and Site-Specific Assembly of Colloids by Particle Lithography. *Langmuir* **2005**, *21*, 4813–4815.
24. Motl, N. E.; Ewusi-Annan, E.; Sines, I. T.; Jensen, L.; Schaak, R. E. Au-Cu Alloy Nanoparticles with Tunable Compositions and Plasmonic Properties: Experimental Determination of Composition and Correlation with Theory. *J. Phys. Chem. C* **2010**, *114*, 19263–19269.
25. Gu, H. W.; Zheng, R. K.; Zhang, X. X.; Xu, B. Facile One-Pot Synthesis of Bifunctional Heterodimers of Nanoparticles: A Conjugate of Quantum Dot and Magnetic Nanoparticles. *J. Am. Chem. Soc.* **2004**, *126*, 5664–5665.
26. Yu, H.; Chen, M.; Rice, P. M.; Wang, S. X.; White, R. L.; Sun, S. H. Dumbbell-like Bifunctional Au-Fe_3O_4 Nanoparticles. *Nano Lett.* **2005**, *5*, 379–382.
27. Erhardt, R.; Zhang, M. F.; Boker, A.; Zettl, H.; Abetz, C.; Frederik, P.; Krausch, G.; Abetz, V.; Muller, A. H. E. Amphiphilic

Janus Micelles with Polystyrene and Poly(methacrylic acid) Hemispheres. *J. Am. Chem. Soc.* **2003**, *125*, 3260–3267.
28. Gentilini, C.; Pasquato, L. Morphology of Mixed-Monolayers Protecting Metal Nanoparticles. *J. Mater. Chem.* **2010**, *20*, 1403–1412.
29. Gentilini, C.; Franchi, P.; Mileo, E.; Polizzi, S.; Lucarini, M.; Pasquato, L. Formation of Patches on 3D SAMs Driven by Thiols with Immiscible Chains Observed by ESR Spectroscopy. *Angew. Chem., Int. Ed.* **2009**, *48*, 3060–3064.
30. Norgaard, K.; Weygand, M. J.; Kjaer, K.; Brust, M.; Bjornholm, T. Adaptive Chemistry of Bifunctional Gold Nanoparticles at the Air/Water Interface. A Synchrotron X-ray Study of Giant Amphiphiles. *Faraday Discuss.* **2004**, *125*, 221–233.
31. Glogowski, E.; He, J. B.; Russell, T. P.; Emrick, T. Mixed Monolayer Coverage on Gold Nanoparticles for Interfacial Stabilization of Immiscible Fluids. *Chem. Commun.* **2005**, 4050–4052.
32. Kubowicz, S.; Daillant, J.; Dubois, M.; Delsanti, M.; Verbavatz, J. M.; Mohwald, H. Mixed-Monolayer-Protected Gold Nanoparticles for Emulsion Stabilization. *Langmuir* **2010**, *26*, 1642–1648.
33. Pickering, S. U. Emulsions. *J. Chem. Soc., Trans.* **1907**, *91*, 2001–2021.
34. Pradhan, S.; Xu, L. P.; Chen, S. W. Janus Nanoparticles by Interfacial Engineering. *Adv. Funct. Mater.* **2007**, *17*, 2385–2392.
35. Kalsin, A. M.; Fialkowski, M.; Paszewski, M.; Smoukov, S. K.; Bishop, K. J. M.; Grzybowski, B. A. Electrostatic Self-Assembly of Binary Nanoparticle Crystals with a Diamond-like Lattice. *Science* **2006**, *312*, 420–424.
36. Jana, N. R.; Peng, X. G. Single-Phase and Gram-Scale Routes toward Nearly Monodisperse Au and Other Noble Metal Nanocrystals. *J. Am. Chem. Soc.* **2003**, *125*, 14280–14281.
37. Cassie, A. B. D.; Baxter, S. Wettability of Porous Surfaces. *Trans. Faraday Soc.* **1944**, *40*, 0546–0550.
38. Saien, J.; Akbari, S. Interfacial Tension of Toluene Plus Water Plus Sodium Dodecyl Sulfate from (20 to 50) Degrees C and pH between 4 and 9. *J. Chem. Eng. Data* **2006**, *51*, 1832–1835.
39. Liu, Y. X.; Jessop, P. G.; Cunningham, M.; Eckert, C. A.; Liotta, C. L. Switchable Surfactants. *Science* **2006**, *313*, 958–960.
40. de Gennes, P. G. Soft Matter. *Science* **1992**, *256*, 495–497.
41. Hyeon, T.; Lee, S. S.; Park, J.; Chung, Y.; Bin Na, H. Synthesis of Highly Crystalline and Monodisperse Maghemite Nanocrystallites without a Size-Selection Process. *J. Am. Chem. Soc.* **2001**, *123*, 12798–12801.